Defected Ground Structure-based Compact Wideband Monopole Antenna Design with Equivalent Circuit Modeling for Communication and Sensing Applications

Mohammad Rabiul Hossen, Mehrab Ramzan and Padmanava Sen
Barkhausen Institut, Dresden, Germany
rabiul.hossen,mehrab.ramzan,padmanava.sen@barkhauseninstitut.org

***Abstract*—In this paper, a compact ultra-wideband (UWB) antenna is designed for communication and sensing applications based on the defected ground structure (DGS) method. Compared to traditional UWB antennas using a thick substrate and circular/elliptical patch, this paper utilises an alternative approach by using a rectangular patch with the finite slotted ground on a 0.508 mm thick RO4003 substrate. A systematic approach is presented for the determination of the slot's position in each step of the DGS method to increase the bandwidth of the narrowband rectangular patch antenna. An equivalent circuit model is also characterized based on the Foster canonical form theorem for the UWB antenna. The fabricated antenna (31.5mm x 33.5 mm) has a bandwidth of 7.9 GHz (3.8-11.7 GHz) with a peak gain of 6 dBi and 90% efficiency in the operating frequency range. Additionally, communication and range measurements are performed to show the future application scenarios like joint communication and sensing (JC&S). Easy identification of the slot position using current distribution for bandwidth enhancement, an equivalent circuit model for simpler theoretical analysis, and experimental system validation of the developed UWB antenna are the highlights of this paper.**

***Index Terms*—DGS, Wideband/UWB, Equivalent Circuit Model, Experimental Validation, JC&S**

I. Introduction

Bandwidth scarcity in wireless communication and radio sensing drew researchers' attention towards new technologies and consumer products utilising them. New research fields like UWB localization/identification, Wi-Fi sensing and upcoming JC&S in 6G could provide solutions to tackle the spectrum scarcity. This way, the currently established communication technology can be used with sensing (e.g. radars) or vice versa to reduce the use of different devices for different applications. UWB technology has the advantages of a high data rate, less interference and greater resistance to multipath fading [1]. For localization, automobile industries are utilizing this large bandwidth (BW) spectrum for precise distance measurement [2]. Therefore, UWB has potential for JC&S applications [3]. In addition, space constraints in battery-driven mobile devices require compact design as most handheld devices are becoming more compact. A wideband compact antenna for UWB applications can address these constraints for such devices. The challenges of achieving large fractional bandwidth and compactness for wideband antenna include the performance parameter trade-offs such as impedance matching bandwidth, maintaining high gain over the frequency span and omnidirectional radiation pattern.

In the literature review, several methods like thick substrate usage, stacked patches, shorting pins, and defected ground structure (DGS) are used to increase the bandwidth (BW) of the planar narrowband microstrip patch antenna [4]–[6]. Defected ground structure method for increasing the BW and impedance matching is more appealing than others due to the compactness of the design. In DGS, defects or slots of different shapes are introduced intentionally in the ground plane. This method reduces size with desired radiation performance [7]. But, this popular technique lacks proper visualization of where to cut the slots. In literature [8]–[11], slots are cut one after another to achieve UWB, and then comparison of S_{11} parameters as well as the current distribution plot of the proposed antenna are shown. But there is no reported information on how the slot's position is determined in each step. Additionally, most of the literature uses one of the below options to design the UWB antenna from a narrowband antenna -

- Using circular or elliptical patches, that provide wider and symmetric modes than rectangular patches due to their resonant behaviour [12], [13].
- Using lossy dielectric material like FR4 and thick substrate for bandwidth enhancement.

Therefore, in this paper, step-wise techniques are given in Section II based on the current distribution analysis to determine the slot position for achieving UWB (3.8-11.7 GHz) from a narrow band patch antenna. Standard RO 4003 (ϵ_r = 3.55) substrate with a moderate thickness of 0.508 mm is used due to its low cost and low losses at high frequencies compared to other cheaper options like FR4. Additionally, an equivalent circuit model is derived for the designed UWB monopole antenna in Section III, which provides useful insights into the

This work is financed on the basis of the budget passed by the Saxon State Parliament.

Copyright © 2023 IEEE.DOI 10.1109/JCS57290.2023.10107460

Copyright © 2023 10.1109/JCS57290.2023.10107460. Personal use of this material is permitted. Permission from IEEE must be obtained for all other uses, in any current or future media, including reprinting/republishing this material for advertising or promotional purposes, creating new collective works, for resale or redistribution to servers or lists, or reuse of any copyrighted component of this work in other works

TABLE I: Narrowband Patch Antenna Dimensions

Parameters	SubL	SubW	Lp	Wp	Lf_50	Wf_50	Lf_qw	Wf_qw
Value (mm)	31.5	33.5	13.5	17	4	1.14	8	0.28

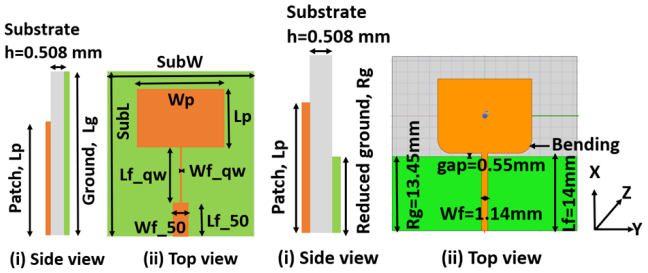

Fig. 1: (a) Narrowband MPA (b) Antenna-1 W/O slot.

design and performance of the antenna. Section IV presents the communication and sensing experiments to show that the developed antenna can be a good candidate for future joint communication and sensing applications. At the end, a comparison table between the references and the proposed antenna is shown.

II. Antenna Design and Results

Resonance frequency plays an essential role in calculating the dimension of the antenna. The dimension of the antenna is inversely proportional to the resonance frequency. Therefore, obtaining an acceptable UWB frequency response from the same narrowband dimension becomes a challenging task. In this section, a narrowband patch antenna is designed first at 5.9 GHz. After that, the DGS method is followed to design the UWB antenna from the same narrowband dimension with the explanation of the slot position determination.

A. Narrowband Microstrip Patch Antenna (MPA)

The microstrip line feeding technique is considered for designing the antenna rather than the inset feeding technique. This causes the antenna to resonate at multiple resonant frequencies for a wideband design. In [4], formulas are given to calculate the dimensions for the narrowband patch antenna. By using these formulas, a narrowband patch antenna is designed at 5.9 GHz, and then step-by-step techniques are employed to increase BW from the same size. Table I and Fig. 1a provide the dimension of the narrowband quarter-wavelength impedance matching patch antenna. Fig. 2 shows the antenna is matched to 5.9 GHz and the BW is 60 MHz.

B. Wideband Monopole Antenna

1) Partial ground and bending effect: The use of a ground plane for the entire substrate below the patch causes the antenna to radiate in the broadside region. To obtain an omnidirectional radiation pattern, a finite ground plane must be used [9]. Also, finite ground planes are capable of supporting multiple resonant modes. Fig. 1b shows the finite ground plane with the rectangular bending shape of the patch antenna-1. Substrate and patch dimensions are kept similar to the previous narrowband design. The quarter-wavelength impedance transformer is removed, and a direct edge feeding microstrip line of 14 mm is used for feeding the antenna. The gap from

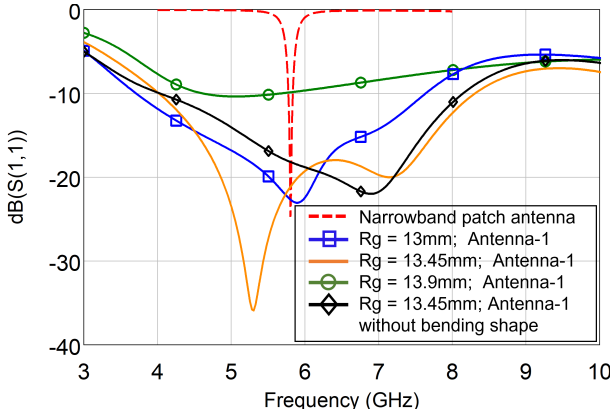

Fig. 2: S_{11} of narrowband patch antenna and parametric analysis of the finite ground length of antenna-1.

the top edge of the ground plane to the bottom edge of the patch plays a significant role in matching the impedance and widening of the antenna BW. The gap of 0.55 mm for the finite ground (Rg=13.45mm) is selected after parametric analysis of antenna-1. In Fig. 2, Rg=13.45mm shows better impedance matching than the Rg=13.45mm without bending shape of the antenna-1. A gap smaller than 0.55 mm starts degrading the impedance matching. The bending shape in the patch tunes the capacitive coupling by increasing the distance between the patch and the ground, improving the impedance matching at 5.3 GHz and 7.1 GHz. The width of the transmission line is kept constant at 1.14 mm for 50 Ω. SMA connector with wave port excitation is used to get the antenna simulations as close as possible to the realistic environment.

2) Different ground slots position effects: Slot addition in the ground plane changes the current distribution, creates additional resonance at a higher frequency and improves the impedance matching [9]. Following that process, different antenna types are designed, as shown in Fig. 3. From Fig. 1b, antenna-1 (without slot) has resonances at 5.6 GHz and 7.1 GHz. Now, to add a new resonance at higher frequencies, current distribution in the ground plane of antenna-1 is studied. Fig. 4a shows the current distribution on the ground plane around the two resonances (5.6 and 7.1 GHz) as well as at 10.3 GHz. The bottom centre edge of the ground plane has high current distribution at 10.3 GHz, 7.1 GHz and 5.6 GHz. Therefore, cutting a slot at the bottom centre edge of the ground will add a resonance at 10.3 GHz, as shown in Fig 5 (Antenna-2). There is a band notch from 7.5 GHz to 9.5 GHz in antenna-2. Therefore, the current distribution is analyzed for antenna-2 to improve the impedance matching, where there is a band notch. Fig. 4b shows that the top edge of the antenna-2 ground plane has high current distribution near the

Copyright © 2023 10.1109/JCS57290.2023.10107460. Personal use of this material is permitted. Permission from IEEE must be obtained for all other uses, in any current or future media, including reprinting/republishing this material for advertising or promotional purposes, creating new collective works, for resale or redistribution to servers or lists, or reuse of any copyrighted component of this work in other works

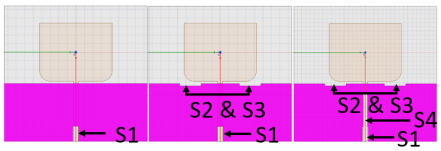

(a) Antenna 2 (Bottom slot) (b) Antenna 3 (Bottom Top slots) (c) Antenna 4 (Bottom Middle Top slots)

Fig. 3: Steps in designing the proposed antenna.

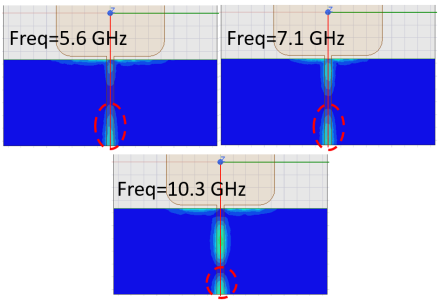

(a)

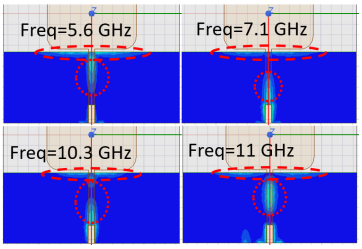

(b)

Fig. 4: Current distribution analysis at different frequencies on the ground plane of (a) antenna-1 (b) antenna-2

TABLE II: Slots Dimensions

Parameters	S1_L	S1_W	S2,3_L	S2,3_W	S4_L	S4_W
Value (mm)	3.45	1.4	8	1	0.5	5

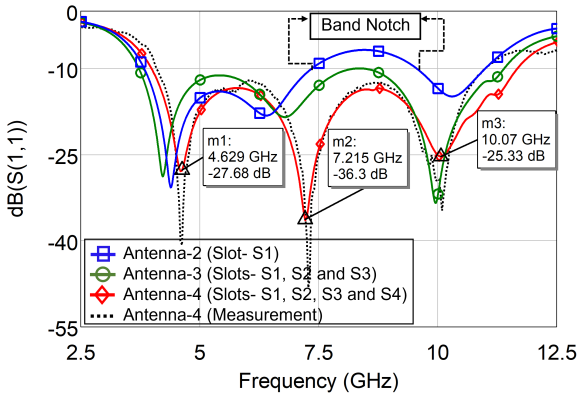

Fig. 5: S_{11} parameters of antennas 2 to 4.

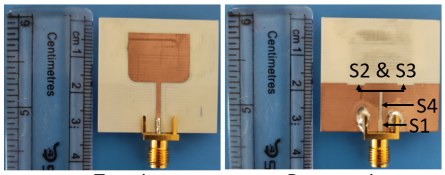

Fig. 6: Fabricated UWB antenna-4 top and bottom view.

patch bending. Therefore, cutting two slots at the top edge of the ground plane of antenna-2 tunes the capacitive reactance. Fig. 5 (Antenna-3) shows that the band notch disappears for antenna-3 from 7.5 GHz to 9.5 GHz. Since the reflection coefficient of antenna-3 is still very close to -10 dB, the current distribution is analyzed again for antenna-2. Fig. 4b shows that the current distribution is also high in the middle of the ground plane. Therefore, placing a slot in the middle of the ground plane brings down the S_{11} significantly below -10 dB, as shown in Fig. 5 (Proposed antenna-4). From Fig 5, the total simulated BW of the proposed antenna-4 is observed from 3.8 GHz to 11.7 GHz, and the measured BW is 3.85 GHz to 11 GHz. The fractional BW has increased to 101.9 % from the narrowband design's 1.03 %. Fig. 6 shows the fabricated proposed UWB antenna-4, and Table II provides all the physical dimensions of the necessary slots in the ground plane. Parametric analysis is used to find the proper size of slots used in the ground plane.

The radiation pattern in E-plane (XZ direction) and H-plane (YZ direction) in Fig. 7 shows that the antenna radiates omnidirectionally. Fig. 8 shows the gain and radiation efficiency,

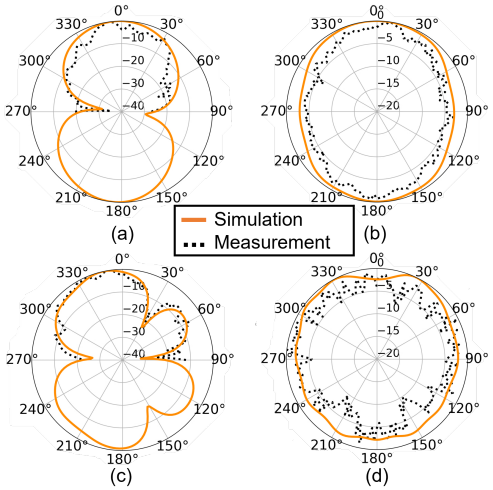

Fig. 7: Normalized radiation pattern (Simulation vs Measurement) (a) E-plane at 7.1 GHz (b) H-plane 7.1 GHz (c) E-plane at 10 GHz (d) H-plane 10 GHz.

Copyright © 2023 10.1109/JCS57290.2023.10107460. Personal use of this material is permitted. Permission from IEEE must be obtained for all other uses, in any current or future media, including reprinting/republishing this material for advertising or promotional purposes, creating new collective works, for resale or redistribution to servers or lists, or reuse of any copyrighted component of this work in other works

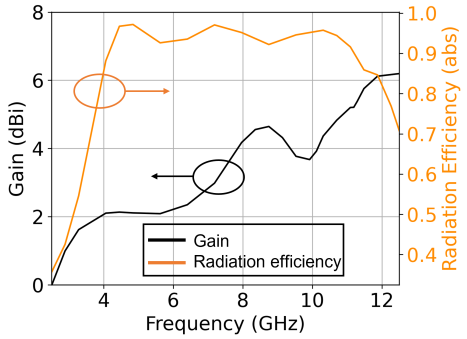

Fig. 8: Simulated gain and radiation efficiency.

where the gain is 2-6 dBi in the operating range and efficiency is above 90%.

III. Equivalent Circuit Model

An antenna can be represented by an equivalent circuit model of lumped elements which carries both theoretical and practical importance. It provides useful insights into the design and performance of the antenna. This paper investigates the equivalent circuit based on the Foster canonical form [14].

1) Equivalent Circuit Based on Foster Canonical Forms: The input impedance of an antenna can be represented by Foster's canonical form, assuming there are no Ohmic losses. The first Foster canonical form in Fig 9a is suitable for modelling "electric antennas", which behaves as an open circuit at DC input signal [15].

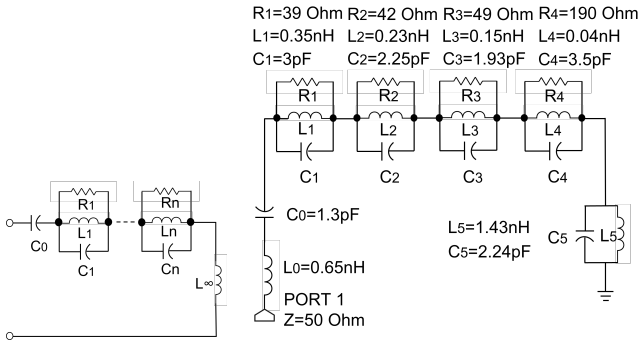

(a) (b)

Fig. 9: (a) Foster first canonical form (b) Equivalent circuit model of the UWB antenna-4.

According to the Foster reactance theorem, around resonance frequency, the antenna behaves as a series RLC circuit where the derivative of the antenna's reactance with respect to frequency is positive. At near anti-resonance ranges, the antenna acts as parallel RLC circuits, and the frequency derivative of the antenna's reactance is negative [15]. In a finite frequency range, when the antenna reactance changes from negative (capacitive) to positive (inductive), the frequency derivative of the antenna reactance is positive and vice versa.

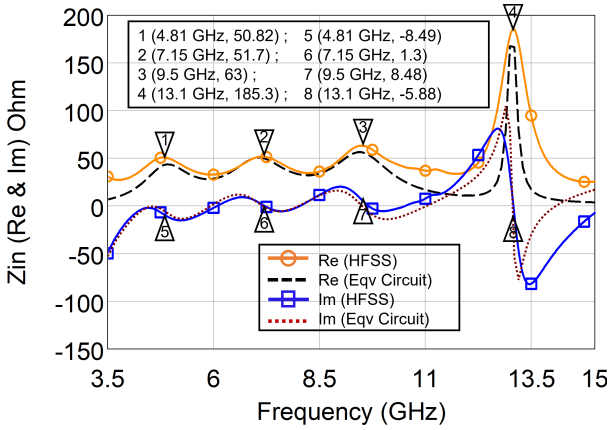

Fig. 10: Input impedance comparison of the equivalent circuit and HFSS simulation of antenna 4.

TABLE III: Element values of the equivalent circuit model of UWB antenna-4.

	Z_n	Z_0	Z_1	Z_2	Z_3	Z_4	Z_5
AWR	R_n (Ω)		39	42	49	190	
	C_n(pF)	1.3	3	2.246	1.93	3.5	2.24
	L_n(nH)	0.65	0.352	0.226	0.146	0.0425	1.425
	f_n(GHz)		4.81	7.15	9.5	13.1	
HFSS	R_n (Ω)		50.82	51.7	63	185.3	
	C_n(pF)	1.425	3.9	11.21	2.63	2.066	-
	L_n(nH)	0.65	0.281	0.045	0.107	0.0715	-
	f_n(GHz)		4.81	7.15	9.5	13.1	

Fig. 10 shows that the input impedance of the UWB antenna-4 and the BW goes through 4 anti-resonances at 4.81 GHz, 7.15 GHz, 9.5 GHz and 13.1 GHz. The equivalent circuit is then represented by four parallel RLC cells connected in series as shown in Fig. 9b for these anti-resonances. C1 and L1 represent the capacitance and inductance of the antenna when operating at the lower resonance frequency. The parallel LC cell is the combined effect of the slots in the antenna's ground. The values of the components in the circuit are tuned to achieve proper matching. Table III presents the element values from the HFSS and achieved tuned values from the AWR for designing the equivalent circuit of the proposed UWB antenna-4.

IV. Communication and Sensing Experiments

This section shows communication and sensing experiments as use cases for the developed UWB antenna.

A. Communication Experiment

The communication experiment setup is shown in Fig. 11a using Keysight Arbitrary Waveform Generator (AWG) M8195A to generate the modulated signal and Keysight UXR0254AP 25 GHz 256 Gsa/s 10 bit Real-Time Oscilloscope to perform the digital demodulation and performance analysis. Measurement is performed in over-the-air (OTA) and direct coaxial cable to compare the performance of 16

Copyright © 2023 10.1109/JCS57290.2023.10107460. Personal use of this material is permitted. Permission from IEEE must be obtained for all other uses, in any current or future media, including reprinting/republishing this material for advertising or promotional purposes, creating new collective works, for resale or redistribution to servers or lists, or reuse of any copyrighted component of this work in other works

QAM over the frequency span of 8.1 GHz. A wideband, high-gain LNA (mini-circuits ZVA-203GX+) is connected after the Rx antenna to facilitate the receiver measurement analysis, as the UWB antenna does not have a very high gain. As expected, the over-the-air SNR (Fig. 11c) is lower compared to the direct cable measurements(Fig. 11b). However,with this measurement, the usability of this antenna across the 8+ GHz frequency range is validated.

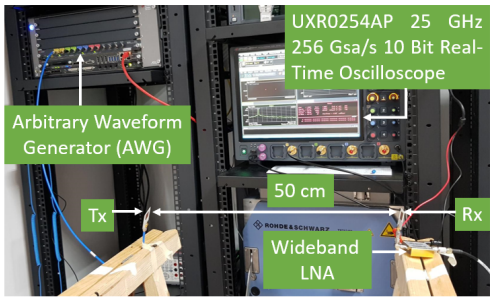

(a)

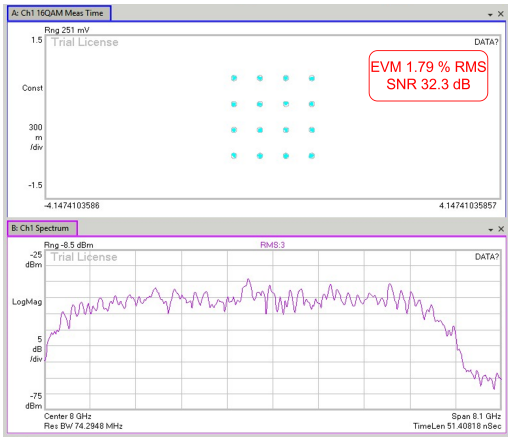

(b)

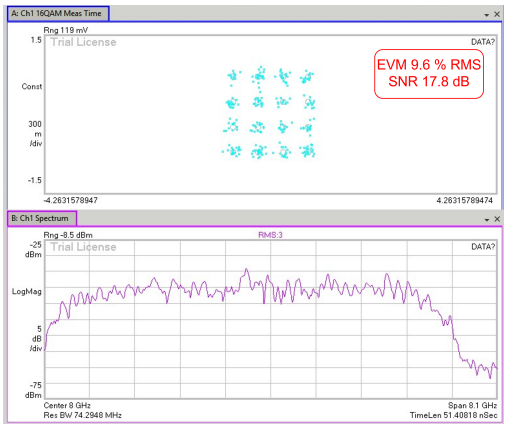

(c)

Fig. 11: (a) Communication measurement setup; Constellation and PSD plot of (b)16 QAM (direct cable) (c) 16 QAM (OTA).

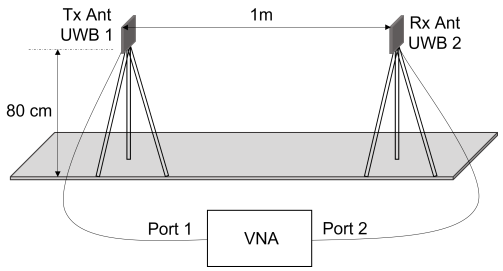

(a)

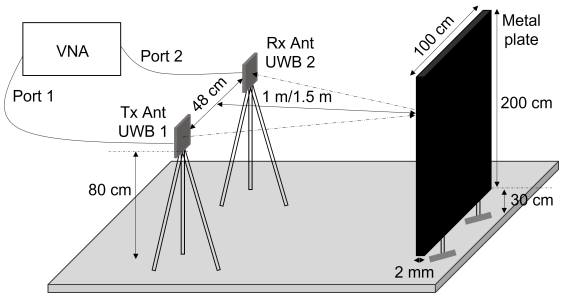

(b)

Fig. 12: Range measurement setup (a)LOS (b) NLOS with metal object.

B. Range Measurement

In this section, the distance between two UWB antennas (LOS) and distance measurement to the metal plate (NLOS) as an object is performed in an anechoic chamber. The power delay profile (PDP) method is used here as a tool to measure the range [16], [17].

1) LOS antenna range measurement: Fig. 12a shows that the fabricated UWB antennas in the line of sight (LOS) configuration setup to measure the distance between the transmitter and receiver. The distance between them is set to 1 m, and height is maintained at 80 cm above the ground. The measured frequency range is set from 3.5 GHz to 12.5 GHz, corresponding to a delay resolution of 111 ps or 0.1 ns and the transmit power is set to 0 dBm. The spectrum is divided into 201 points. Therefore, the maximum excess delay or maximum measurable time-domain delay window is 2.22 ns. Inverse Fast Fourier Transform (IFFT) is applied to the measured complex S_{21} data to obtain the time-domain channel impulse response. After that, a Hamming window reduces the side lobe level in the delay domain. The PDP is calculated using equation $P(\tau) = E[|h(t,\tau)|^2]$ from channel impulse response [18]. Finally, the horizontal delay axis is converted to the distance axis to show the LOS range between the transmitter and receiver. Fig. 13a indicates that the peak received signal power is at 1.07 m, which is the distance between the antennas.

2) Metal Plate Distance Measurement (NLOS Antenna): A metal plate (200 cm x 100 cm x 2 mm) is used as an object, where both UWB antennas are placed side by side in a sensing experiment, as shown in Fig. 12b. The distance between the antennas is 48 cm, and from the antenna's center point to

Copyright © 2023 10.1109/JCS57290.2023.10107460. Personal use of this material is permitted. Permission from IEEE must be obtained for all other uses, in any current or future media, including reprinting/republishing this material for advertising or promotional purposes, creating new collective works, for resale or redistribution to servers or lists, or reuse of any copyrighted component of this work in other works

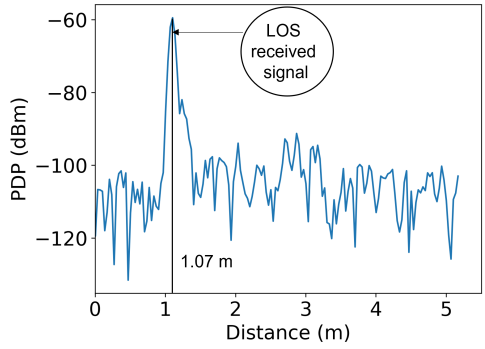

(a)

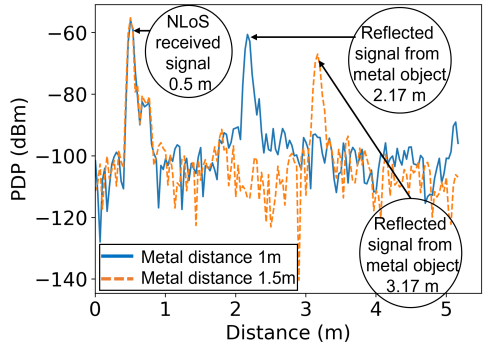

(b)

Fig. 13: Range measurement using PDP (a) LOS (b) NLOS with metal object.

the metal plate varies 1 m to 1.5 m during measurements 1 and 2. Fig. 13b shows that for each distance measurement, there is a common peak at 0.5 m which is the NLOS received signal of the antenna due to the omnidirectional radiation behaviour. The other peak is at 2.17 m and 3.17 m, which is the round trip distance reflected from the metal object presence in measurements 1 (1 m) and 2 (1.5 m), respectively, received by the receiver antenna.

V. Conclusion

Bandwidth enhancement using DGS is a popular and known method for UWB antenna design. But most of the literature lacks information about determining the slot position. This paper shows the determination of the slot's position in each step of the DGS method to increase the BW of the narrowband patch antenna. The current distribution magnitude plot in the ground plane at a particular desired frequency gives absolute information about the position of the slot. Cutting slots at that high current area creates new resonance(s) as well as improves the impedance matching. The proposed UWB antenna has a peak gain of 6 dBi at 11.7 GHz and a BW of 7.9 GHz (3.8-11.7GHz). The fractional BW has been increased to 101.9 % from the 1.03 % of the narrowband design. An equivalent circuit model is also developed in AWR for the fabricated UWB antenna based on the Foster first canonical form, which matches the input impedance of the simulated UWB antenna. In addition, communication and sensing experiments are performed to show that this antenna can be a good candidate for futuristic applications like joint communication and sensing. A comparison between the proposed and reference UWB antennas is given in Table IV.

References

[1] FCC F. report and order, revision of part 15 of the commission's rules regarding ultra-wideband transmission systems. FCC02-48, April. 2002 Apr.
[2] Digital Key Release 3.0 specification; https://carconnectivity.org/press-release/car-connectivity-consortium-delivers-digital-key-release-3-0-specification/
[3] Fettweis G, Schlüter M, Thomä R, Boche H. Joint Communications & SensingJoint Communications & Sensing: Common Radio-Communications and sensor technolog. VDE ITG. 2021:24.
[4] Garg R, Bhartia P, Bahl IJ, Ittipiboon A. Microstrip antenna design handbook. Artech house; 2001.
[5] Kumar G, Ray KP. Broadband microstrip antennas. Artech house; 2003.
[6] Rawat S, Sharma KK. A compact broadband microstrip patch antenna with defective ground structure for C-Band applications. Central European Journal of Engineering. 2014 Sep;4(3):287-92.
[7] Weng LH, Guo YC, Shi XW, Chen XQ. An overview on defected ground structure. Progress In Electromagnetics Research B. 2008;7:173-89.
[8] Ojaroudi N, Ojaroudi M, Ghadimi N. UWB omnidirectional square monopole antenna for use in circular cylindrical microwave imaging systems. IEEE Antennas and Wireless Propagation Letters. 2012 Nov 27;11:1350-3.
[9] Waghmare C, Kothari A. Spanner shaped ultra wideband patch antenna. In2014 Students Conference on Engineering and Systems 2014 May 28 (pp. 1-4). IEEE.
[10] Wang L, Wu W, Shi XW, Wei F, Huang Q. Design of a novel monopole UWB antenna with a notched ground. Progress In Electromagnetics Research C. 2008;5:13-20.
[11] Lu Y, Huang Y, Chattha HT, Cao P. Reducing ground-plane effects on UWB monopole antennas. IEEE Antennas and Wireless propagation letters. 2011 Feb 24;10:147-50.
[12] Panda DC, Patro TJ. Resonant frequency of Egg shaped microstrip antenna. In2017 IEEE Applied Electromagnetics Conference (AEMC) 2017 Dec 19 (pp. 1-2). IEEE.
[13] Perli BR, Rao AM. Analysis of microstrip patch antenna with loading slot using characteristic modes. In2020 7th International Conference on Smart Structures and Systems (ICSSS) 2020 Jul 23 (pp. 1-4). IEEE.
[14] Foster RM. A reactance theorem. Bell System technical journal. 1924 Apr;3(2):259-67.
[15] Wang SB, Niknejad AM, Brodersen RW. Circuit modeling methodology for UWB omnidirectional small antennas. IEEE Journal on Selected Areas in Communications. 2006 Apr 10;24(4):871-7.
[16] Xie Y, Li Z, Li M. Precise power delay profiling with commodity Wi-Fi. IEEE Transactions on Mobile Computing. 2018 Jul 30;18(6):1342-55.
[17] Wu K, Xiao J, Yi Y, Gao M, Ni LM. FILA: Fine-grained indoor localization. In2012 Proceedings IEEE INFOCOM 2012 Mar 25 (pp. 2210-2218). IEEE.
[18] Rappaport TS. Wireless communications: principles and practice. New Jersey: prentice hall PTR; 1996 Jan 15.

Copyright © 2023 10.1109/JCS57290.2023.10107460. Personal use of this material is permitted. Permission from IEEE must be obtained for all other uses, in any current or future media, including reprinting/republishing this material for advertising or promotional purposes, creating new collective works, for resale or redistribution to servers or lists, or reuse of any copyrighted component of this work in other works

TABLE IV: Comparison Between Proposed and Reference UWB Antennas.

Ref No.	Patch shape	Size (mm)	Gain (dBi)	η	Fractional BW(%)	Circuit model	Advantages/Disadvantages
[8]	Square	12x18x1.6	-	86%	126.1	-	(a) FR4 substrate with 1.6 mm thickness (b) Compact but too many slots with no explanation behind the slot's position
[9]	Elliptical	45x45x1.6	3.54	-	135.2	-	(a) FR4 substrate with 1.6 mm thickness (b) Large dimension (c) Lower gain
[10]	Circular	45x40x1.5	5.5	-	137.1	-	(a) FR4 substrate with 1.5 mm thickness (b) Large dimension (c) Good gain but no explanation behind the slot's position
[11]	Elliptical	35x32x1.5	4.4	-	118.8	Yes	(a) Elliptical shape with FR4 substrate and 1.5 mm thickness (b) No explanation behind the slot's position
Proposed design	Rectangular	31.5x33.5x 0.508	6	90%	101.9	Yes	(a) Good gain and high efficiency (b) Easy slot position determination in each step of BW enhancement (c) Eqv circuit model (d) Application use case studies